AAPT PHYSICS EDUCATION | AMERICAN JOURNAL of PHYSICS

Damped oscillations and equilibrium in a mass-spring system subject to sliding friction forces: Integrating experimental and theoretical analyses

P. Onorato, D. Mascoli, and A. DeAmbrosis

Citation: Am. J. Phys. **78**, 1120 (2010); doi: 10.1119/1.3471936
View online: http://dx.doi.org/10.1119/1.3471936
View Table of Contents: http://ajp.aapt.org/resource/1/AJPIAS/v78/i11
Published by the American Association of Physics Teachers

Related Articles

Improving the quantification of Brownian motion
Am. J. Phys. 81, 485 (2013)

Photon charge experiment
Am. J. Phys. 81, 436 (2013)

Collimated blue light generation in rubidium vapor
Am. J. Phys. 81, 442 (2013)

The Wiimote on the Playground
Phys. Teach. 51, 272 (2013)

Helicopter Toy and Lift Estimation
Phys. Teach. 51, 310 (2013)

Additional information on Am. J. Phys.

Journal Homepage: http://ajp.aapt.org/
Journal Information: http://ajp.aapt.org/about/about_the_journal
Top downloads: http://ajp.aapt.org/most_downloaded
Information for Authors: http://ajp.dickinson.edu/Contributors/contGenInfo.html

ADVERTISEMENT

Damped oscillations and equilibrium in a mass-spring system subject to sliding friction forces: Integrating experimental and theoretical analyses

P. Onorato
Department of Physics "A. Volta" and Centro di Ricerca Interdipartimentale per la Didattica e la Storia delle Scienze, University of Pavia, Via Bassi 6, I-27100 Pavia, Italy and Laboratori Nazionali di Frascati, INFN, P.O. Box 13, 00044 Frascati, Italy

D. Mascoli and A. DeAmbrosis
Department of Physics "A. Volta" and Centro di Ricerca Interdipartimentale per la Didattica e la Storia delle Scienze, University of Pavia, Via Bassi 6, I-27100 Pavia, Italy

(Received 20 November 2009; accepted 8 July 2010)

Students have difficulty in understanding friction and its associated phenomena. Introductory university courses usually fail to give the topic the attention it deserves and to emphasize the crucial role of friction in establishing mechanical equilibrium as motion ceases. We present an experimental and a theoretical analysis of the periodic motion of a mass-spring system subject to static and kinetic friction forces. Our analysis takes into account the effects of the static friction force on the final mass position. © *2010 American Association of Physics Teachers.*
[DOI: 10.1119/1.3471936]

I. INTRODUCTION

Students have difficulty in understanding friction phenomena,[1] and activities have been proposed to overcome some of their main difficulties.[2] The aim of this paper is to provide an experimental and a theoretical analysis of the role of static and kinetic friction in an oscillating mass-spring system.

Previous papers have studied such systems theoretically.[3–9] In this paper, we use an integrated approach to relate analytical and numerical solutions to the experimental results and observations obtained by students. Students can observe the strong dependence of the final position of a block on the initial conditions and recognize the linear decay of oscillations from graphs obtained using motion sensors. The interpretation of these experimental results motivates the theoretical analysis of the system at various levels. As a result of this analysis, students develop an understanding of how static and kinetic friction forces act and how the cessation of motion is due to the interplay of the two forces. The experiments have been tested with groups of volunteer high school students as part of a collaborative program involving our department and the regional school district.

II. DAMPING AND STOPPING: THE DOUBLE ROLE OF KINETIC AND STATIC FRICTION FORCES

A mass-spring system with mass m and spring constant k is constrained to oscillate on an inclined plane (inclined at the angle θ) in the presence of static and kinetic friction forces, $\mathbf{F}_s$ and $\mathbf{F}_k$, respectively. The magnitude of the kinetic friction force is

$$|\mathbf{F}_k| = \mathrm{sign}(\dot{x})\mu_k|\mathbf{N}|, \tag{1}$$

where $\mathbf{N}$ is the normal force and $\mathrm{sign}(\dot{x})$ denotes the sign function that takes into account the dependence of the kinetic friction force on the direction of the velocity.

If the forces are projected onto an axis parallel to the plane of oscillation and pointed downward (see Fig. 1), Newton's law can be written as

$$m\ddot{x} = -k(x-\bar{x}) - \mathrm{sign}(\dot{x})\mu_k mg\cos\theta + mg\sin\theta, \tag{2}$$

where μ_k is the kinetic friction coefficient, $\bar{x}$ defines the position of the mass when the spring is in its relaxed state, and mg is the magnitude of the gravitational force. Although the magnitudes of the normal and tangential components of the gravitational force are constant, Eq. (2) highlights the periodic alternation of the direction of the dynamic friction force after each half period of motion $T/2=\pi\sqrt{m/k}$. The position of the mass where the spring restoring force counterbalances the tangential component of the weight is $x_g = mg\sin\theta/k + \bar{x}$. Thus, in the absence of friction, x_g represents the center of oscillation and the position of stable equilibrium where the mass remains at rest.

If we assume $x_g=0$ and let $x_0 \neq 0$ represent the initial position of the mass ($\dot{x}_0=0$), we find according to Eq. (2) that the condition necessary for motion is $|\mathbf{F}_{\mathrm{spring}}| > |\mathbf{F}_s|$, that is,

$$k|x_0| > \mu_s mg\cos\theta. \tag{3}$$

This condition allows us to determine the range for which the static friction force exceeds the elastic force, a region corresponding to the positions $x_0 \in [-x_s, +x_s]$ with $x_s = \mu_s mg\cos\theta/k$.

If $|x_0| > x_s$, oscillatory motion is governed by Eq. (2). Suppose that $x_0 > x_s > 0$. In the first half period, Eq. (2) has the form

$$m\ddot{x} = -k(x-\bar{x}) + \mu_k mg\cos\theta + mg\sin\theta, \tag{4}$$

where both the magnitude and the direction of the kinetic friction force are constant in time, and the latter points downward, that is, opposite to the upward direction of the velocity. The solution is

$$x(t) = (x_0 - x_c)\cos(\omega t) + x_c, \tag{5}$$

with $\omega = 2\pi/T$ and $x_c = \mu_k mg\cos\theta/k$. Due to the presence of the constant kinetic friction force, x_c is the position where the net force on the mass is zero, that is, x_c is the center of motion of the first half oscillation. The position where $\dot{x}(T/2)=0$ can be calculated from Eq. (5),

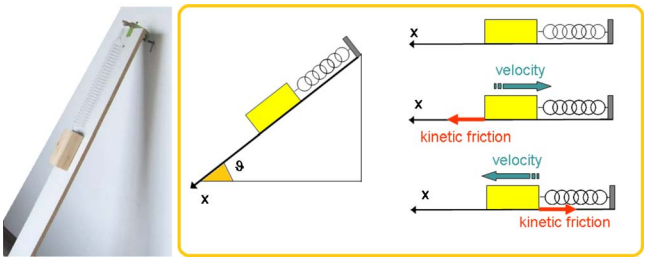

Fig. 1. The mass-spring system. The kinetic friction force and velocity are sketched to show the dependence of the direction of the friction force on the direction of the velocity.

$$x_1 = -x_0 + 2x_c. \tag{6}$$

If we assume $|x_1| > x_s$, there is a change in the direction of the velocity in the next half period and, consequently, in the direction of the kinetic friction force. Thus, the solution of Eq. (2) becomes

$$x(t) = (x_1 + x_c)\cos(\omega t) - x_c, \tag{7}$$

where $-x_c$ is the new oscillation center, which is symmetrical with respect to x_g. The position of the mass after one period is then

$$x_2 = -x_1 - 2x_c = x_0 - 4x_c. \tag{8}$$

The nth-amplitude at the nth-half period is

$$x_n = \begin{cases} (-1)^n(x_0 - 2nx_c) & \text{if } x_0 > x_s > 0 \\ (-1)^n(x_0 + 2nx_c) & \text{if } x_0 < -x_s < 0. \end{cases} \tag{9}$$

Equation (9) demonstrates that the damping of the amplitude is linear, according to the condition that $|x_n| - |x_{n-1}| = -2x_c$ after each half cycle. Equation (9) allows us to derive a constraint on n, where n is an integer representing the number of half oscillations completed by the mass before it comes to rest.

We next discuss the case for which the initial position is located in a region where the elastic force exceeds the static friction force. We assume that $|x_0| > x_s$. The mass comes to rest at x_n after completing nth-half oscillations, that is,

$$|x_n| \le x_s \quad \text{and} \quad |x_{n-1}| > x_s. \tag{10}$$

From Eq. (10) together with Eq. (9), we can deduce the constraint on n,

$$\frac{1}{2}\frac{|x_0| - x_s}{x_c} \le n < \frac{1}{2}\frac{|x_0| - x_s}{x_c} + 1. \tag{11}$$

It is thus possible to quantify the dependence of the final position x_n on the initial position x_0 (with $\dot{x}_0 = 0$). A plot of x_n versus x_0 is given in Fig. 2. The plot is divided into regions corresponding to different numbers of half oscillations completed by the mass before it comes to rest.

If $-x_s \le x_0 \le x_s$, the mass does not oscillate. This central region represents the static region of stable equilibrium where the final position x_n coincides with x_0. The two regions corresponding to $n=1$ of width $2x_c$ represent the range of final positions after one half oscillation. We can estimate both the static and dynamic friction coefficients for a given system by determining the gap $2x_s - 2x_c$ between the two slanted lines in Fig. 2, together with the value of the ratio,

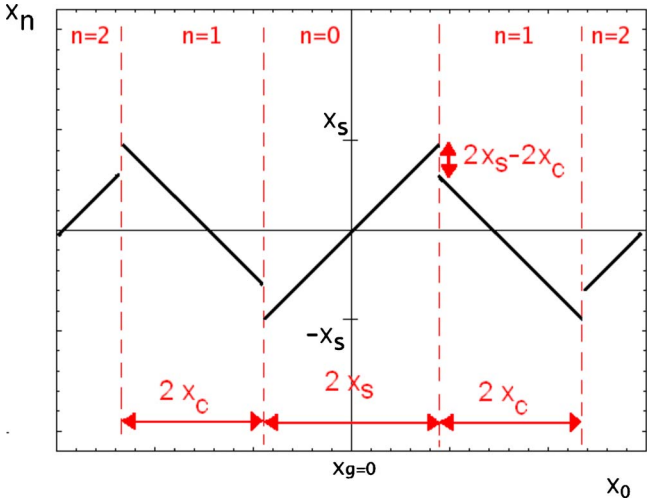

Fig. 2. The final block position x_n for different initial positions x_0 of a damped harmonic oscillator in the presence of both static and sliding friction forces. Regions corresponding to different integer numbers n of half oscillations are highlighted by vertical dashed lines. The gap $2x_s - 2x_c$ between the black lines together with the value of x_c/x_s allows the static and the dynamic friction coefficients to be estimated. The slope of the lines is 1.

$$\frac{x_c}{x_s} = \frac{\mu_k}{\mu_s}. \tag{12}$$

III. THE EXPERIMENTAL APPROACH

The experimental mass-spring system consists of a block with four small plastic supports underneath. The block is attached to a spring fixed at the top of an inclined melanine-coated wooden plane (see Fig. 1). It is possible to use other materials for the block and plane. Some constraints should be taken into account in the choice of materials. If the kinetic friction is too large, few oscillations occur and linear damping is not evident. Also if the static friction is too small, the range in which the static friction force exceeds the elastic force (static region) is greatly reduced and a measurement of the final versus initial position would require too much precision. If the kinetic friction is too small, the effects of viscous friction cannot be disregarded. In practice, we have found that a good set of parameters includes kinetic friction coefficient $\mu_k \approx 0.25$, static friction coefficient $\mu_s \gtrsim \mu_k$, and inclination angle $\theta \approx 1.4$ rad.

A. Evaluating the parameters of the system: A measurement of the static and kinetic friction coefficients

We first describe how to measure the friction coefficients of the block-spring system. Because the direction of the kinetic friction force depends on the direction of the velocity, the kinetic friction coefficient μ_k can be evaluated by measuring the difference between the ascending and the descending accelerations a_a and a_d. From Newton's equations, we can write

$$a_a = g \sin\theta + \mu_k g \cos\theta \quad (v_a < 0), \tag{13}$$

$$a_d = g \sin\theta - \mu_k g \cos\theta \quad (v_d > 0). \tag{14}$$

Therefore,

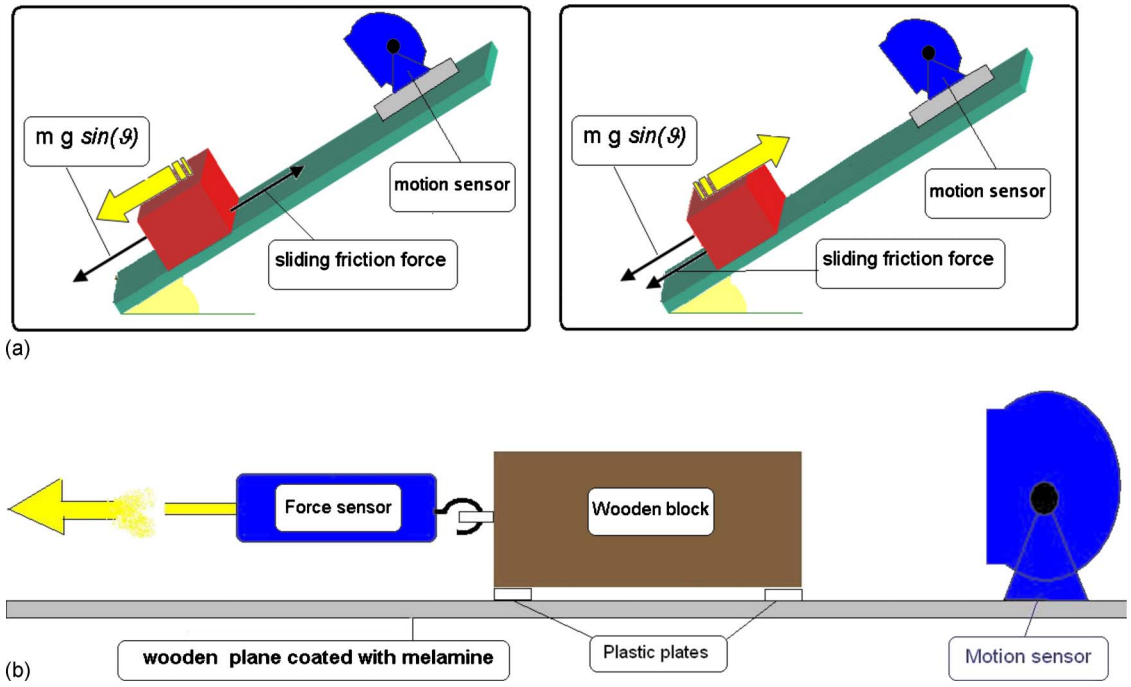

Fig. 3. (a) Experimental approach to estimate the dynamic friction coefficient μ_k. (b) Measurement of the threshold value of the force needed to produce the motion of the block. Measurements are performed by placing the wooden plane horizontally. Both a force sensor attached to the block and a motion sensor are used.

$$\mu_k = \frac{a_a - a_d}{a_a + a_d} \tan\,\theta. \tag{15}$$

The block is pushed from the bottom to the top of the inclined wooden plane and the upward and downward motions are registered by a motion sensor placed at the top of the plane, as shown in Fig. 3(a). The sensor is connected to the computer by a Pasco interface and uses DATASTUDIO software.[10]

Measurements of the position and velocity versus time are shown in Fig. 4. The motion consists of two uniformly accelerated motions (the upward and downward) with different accelerations. From Eq. (15), we obtain the value of the kinetic friction coefficient μ_k,

$$\mu_k = 0.25 \pm 0.03. \tag{16}$$

To determine the value of the static friction coefficient μ_s, we measure the maximum value of the static friction force F_s for various values of the normal force. We vary the normal force by adding known masses on the top of the block. We employ both a force and a motion sensor, as shown in Fig. 3(b). Figure 5 shows the various values of $(mg\,\cos\,\theta, F_s)$ that were collected.

The linear relation between the normal force $mg\,\cos\,\theta$ and the static friction force F_s allows us to estimate the value of μ_s by the statistical interpolation of the experimental data. We find that

$$\mu_s = 0.32 \pm 0.01. \tag{17}$$

From our previous results, we obtain

$$\frac{\mu_k}{\mu_s} = 0.8 \pm 0.1. \tag{18}$$

B. Damping due to the kinetic friction force

To study the motion of the spring-block system, we choose an appropriate inclination angle so that the system will perform a sufficient number of oscillations (in our case $\theta \approx 1.4$ rad). We choose the initial position x_0 (with $\dot{x}_0 = 0$) outside the static region and record the position of the block by means of a motion sensor placed at the bottom of the inclined wooden plane [see Fig. 6(a)].

Figure 6 shows a plot of position versus time; in Fig. 6(b) two centers of oscillation are evident, which are symmetrical with respect to $x_g = 1$ m. If we assume x_g is the origin of the coordinate system, then the two centers of oscillation are at $x_c \sim \pm 0.013$ m. According to the relation $x_c = \mu_k mg\,\cos\,\theta/k$, this value of x_c corresponds to a value of $\mu_k \sim 0.25 \pm 0.05$. The experimentally determined amplitude decay is consistent with Eq. (9); that is, in each half cycle, $|x_n| \sim |x_{n-1}| - 2x_c$. It is also possible to verify that the number of half oscillations before the system comes to rest is consistent with the theoretical predictions. For example, if we choose $x_0 \approx -0.15$ m, six half oscillations occur before motion ceases. This value corresponds to the result derived from Eq. (11), that is, to the first integer number in the range $5.1 \leq n < 6.1$, where Eqs. (12) and (18) have been used to determine the value of x_s. According to Eq. (9), motion should cease at the position corresponding to $n = 6$, that is, at $x_6 \approx 0.006$ m, which agrees with the experimental results [see Fig. 6(b)].

It is also possible to compare the theoretical results shown in Fig. 2 with the experimental values. To this end, the motion sensor was used to record several sets of initial and final position data. For these measurements, the angle of the inclined wooden plane was reduced to $\theta \approx 1$ rad to obtain larger values of x_s and x_c. We increased the number of ex-

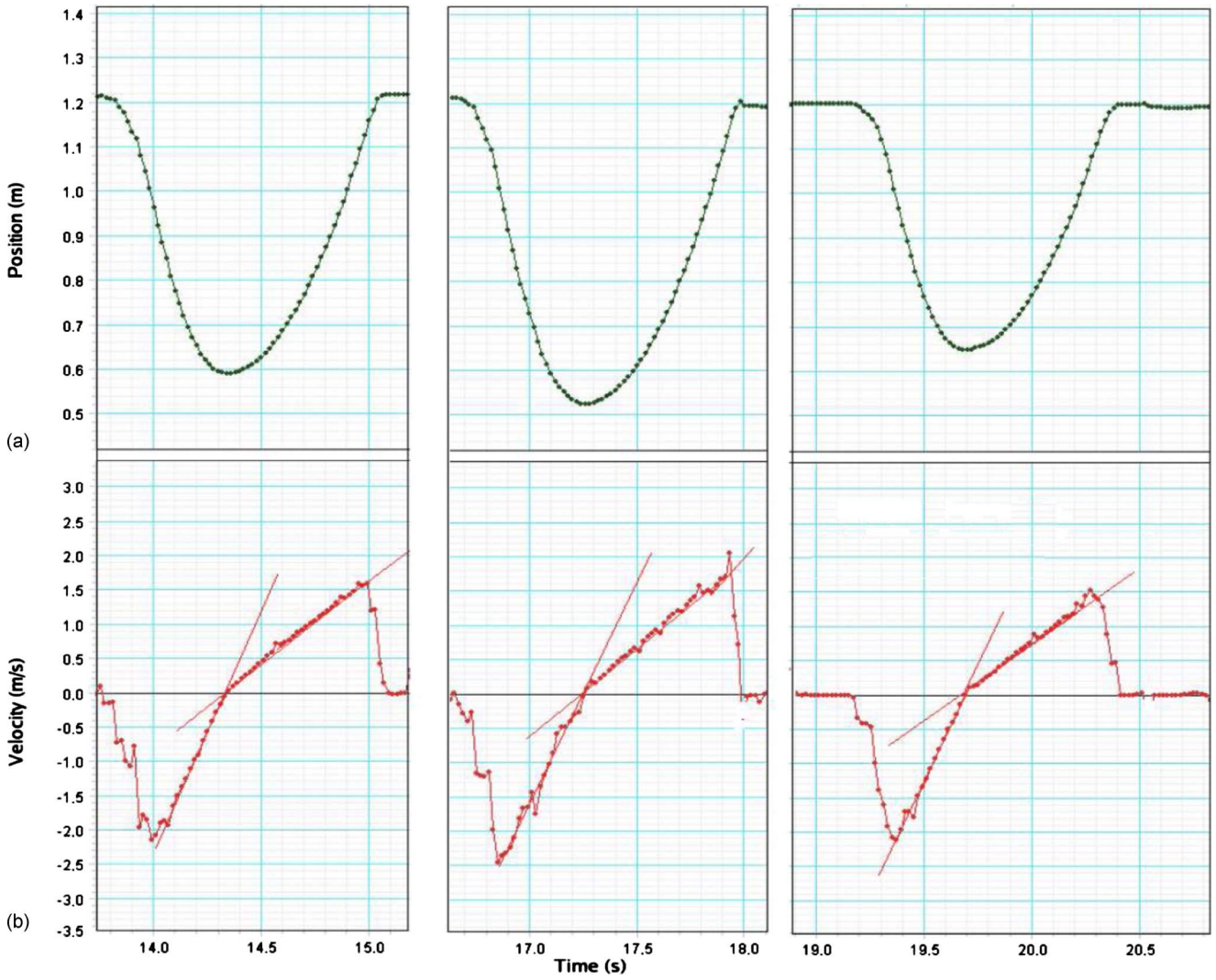

Fig. 4. Measurements of the (a) position and (b) velocity of the block during upward and downward motion. The block is pushed from the bottom to the top of the inclined wooden plane, and a motion sensor records its position and velocity. The sensor is placed at the top. The linear interpolating curves (continuous lines) in the velocity versus time plot allow us to obtain the mean acceleration in each part of motion from the fit parameters. This method reduces the large experimental errors present in the acceleration versus time graphs obtained by the software.

perimental points to compare with the theoretical predictions in Fig. 2. The results are shown in Fig. 7. The qualitative agreement with Fig. 2 is very good. Two discontinuous lines appear, representing two regions of x_0 values. In the first region, the block is unable to oscillate (the static region of stable equilibrium positions); in the second region, it is able to complete one-half of an oscillation.

In Fig. 7 we can also see the range of x_0 values for which the block can complete the second half of the oscillation. The slope obtained by the linear fit of the data in the $n=1$ region agrees with the predicted value. The measured values of x_c and x_s are $x_s=0.049\pm0.002$ m and $x_c=0.043\pm0.002$ m. From Eq. (12), we have $x_c/x_s=\mu_k/\mu_s=0.9\pm0.1$, which is consistent with the value calculated in Eq. (18).

A detailed comparison between the predictions and the experimental results can also be done using the phase space representation. Figure 8(a) shows the velocity versus the position of the oscillator calculated in the presence of both static and kinetic friction forces. Continuous vertical lines at $\pm x_c$ identify the positions of both symmetrical centers of the oscillatory motion. According to Eqs. (5) and (7), for each

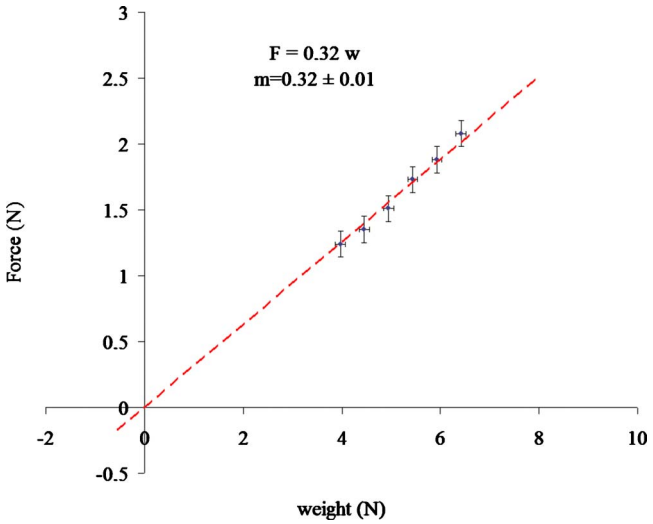

Fig. 5. Static friction coefficient μ_s estimated from the linear relation between $mg\cos\theta$ and F_s defined as the threshold force value before the motion starts. The values of μ_s and μ_k are obtained by the statistical interpolation of the experimental data.

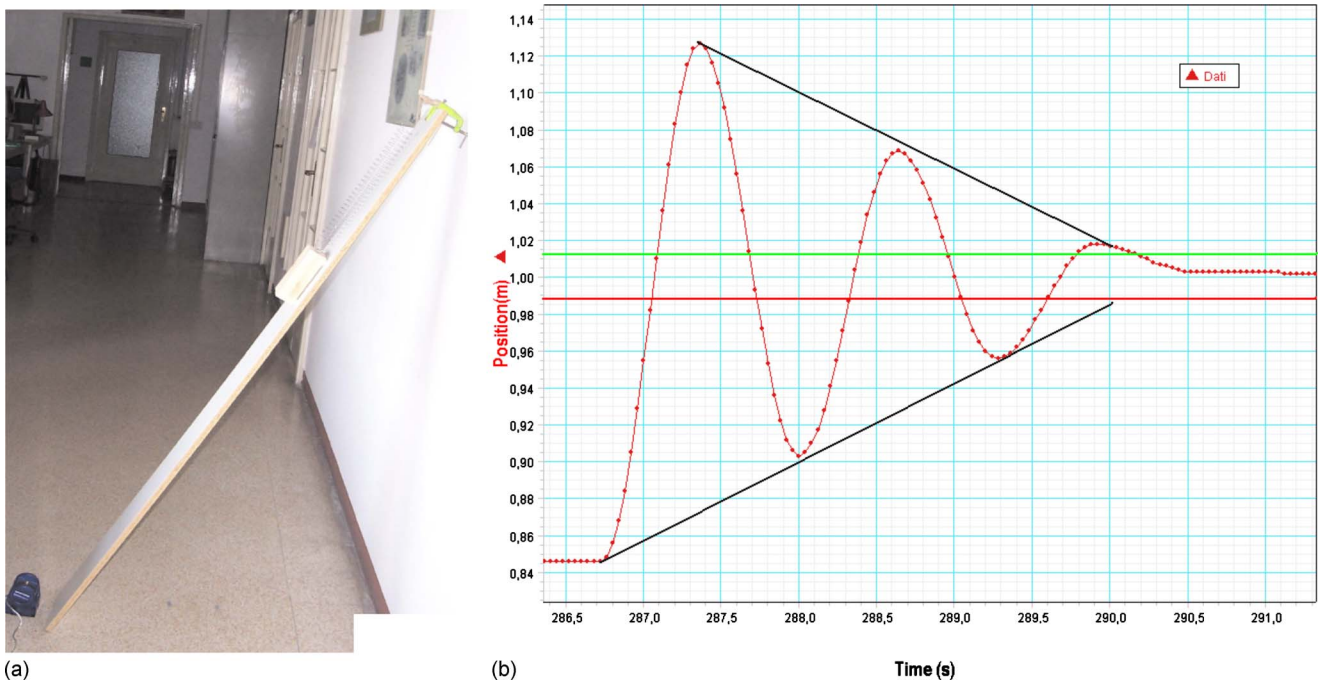

Fig. 6. (a) The apparatus for obtaining periodic damped motion consists of a block-spring system placed on a inclined wooden plane and a motion sensor at the bottom. Four small plastic supports are placed beneath the block. (b) Position versus time for a damped harmonic oscillator in the presence of a static and a kinetic friction force. Continuous tilted lines show the linear amplitude decay. Continuous horizontal lines highlight the presence of two centers at $x_c \sim \pm 0.013$ m symmetrical with respect to the position $x_g = 1$ m for each half period depending on the direction of the motion. Oscillatory motion ends after six half oscillations at $x_6 \sim 0.006$ m.

half oscillation of duration $T/2$, $\pm x_c$ represents the center of the nth-half oscillation, depending on the sign of x_{n-1} corresponding to zero velocity. The other vertical lines at $\pm x_s$ mark the limits of the static region, that is, the region where the static friction force exceeds the elastic force. Figure 8(b) contains a comparison of theory with experiment. The points represent the experimental phase space diagram (obtained with DATASTUDIO). The dashed black line represents the theoretical phase space diagram with the same set of friction parameters as the experimental system. All six half oscillations are clearly visible, and there is good agreement between the experimental and the numerical data [see Fig. 6(b) for a more detailed comparison].

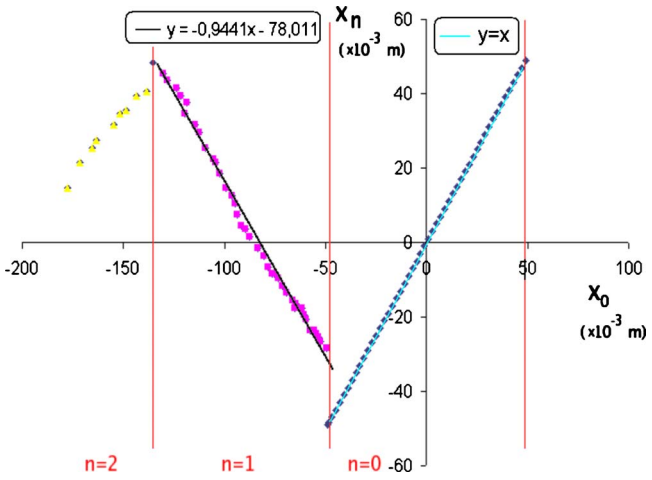

Fig. 7. The final position x_n versus the initial position x_0 in the presence of static and kinetic friction forces. Both positions are recorded by the motion sensor at the bottom of the inclined wooden plane. Regions corresponding to different integer number n of half oscillations are separated by vertical lines. Experimental points are placed on two discontinuous lines as highlighted by a linear fit in the region of $n=1$; the slope is close to 1, as expected. The values obtained for the width of the first two regions are $2x_s = 0.098 \pm 0.004$ m and $2x_c = 0.086 \pm 0.004$ m.

C. Using the experiments with students

The experiments were performed by groups of selected high school students involved in The Undergraduate Degrees in Science Project (Progetto Lauree Scientifiche), whose goal is to attract students to study science at the university level. The students did the experimental activities in groups of three or four and completed the experimental work in two sessions of 2 h each. They had previously performed laboratory work in mechanics and were capable of operating the microcomputer-based laboratory sensors. The students investigated the motion of a wooden block along an inclined plane by focusing on the effects of the kinetic friction force. They also measured the kinetic friction coefficient as reported in Sec. III A. The students subsequently studied the motion of the spring-block system on an inclined wooden plane. They were first asked to predict the nature of a plot of the motion of an undamped oscillator in the t, x, t, v, and x, v planes. Then the experiment described in Sec. III was carried out, and students compared their experimental results to their predictions. Most of the students identified the kinetic friction force as the main cause of damping. A measurement (and a t,x graph) of the middle points of each half oscillation, corresponding to the upward and downward motions, allowed the students to identify the presence of two centers of oscillation. This analysis was very effective in helping students understand the role of kinetic friction in determining the shift of the center of oscillation. Then the range of positions cor-

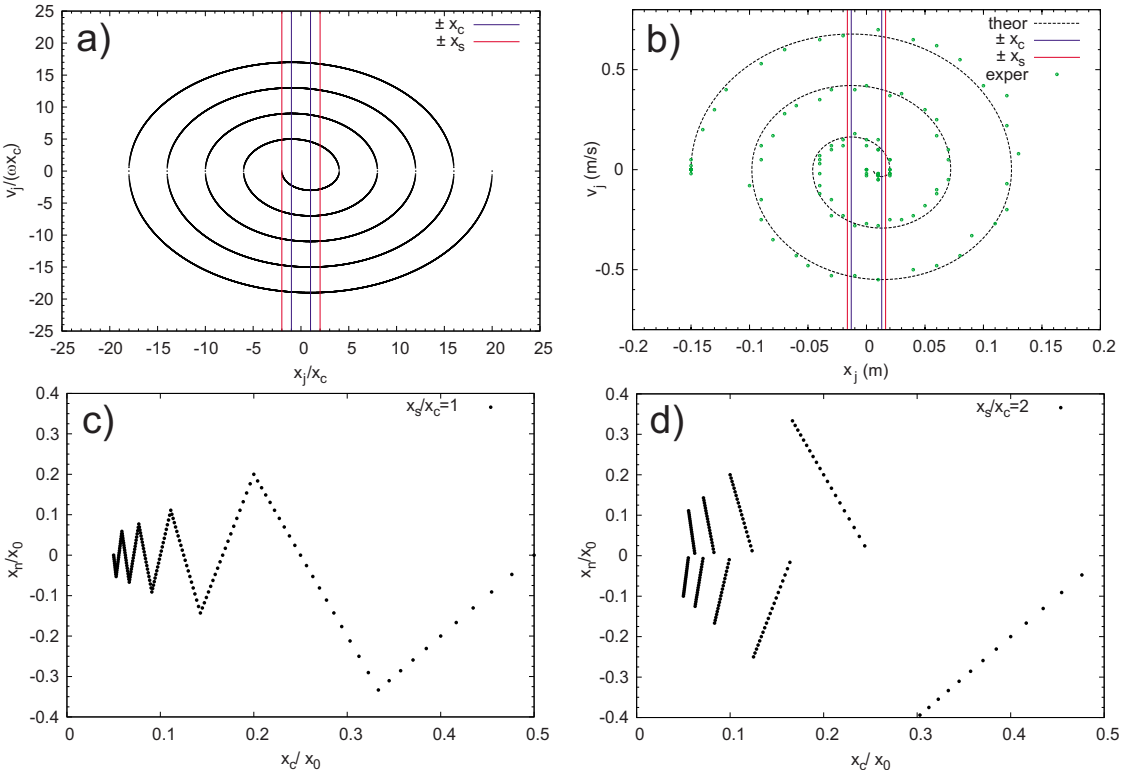

Fig. 8. (a) Phase space representation (the x_j-v_j plane, where x_j and v_j are the oscillator position and velocity at the jth step, respectively) generated by the code for $\mu_s/\mu_k=2$. The continuous vertical lines represent the two oscillation centers $\pm x_c$, and the static region is delimited by vertical dashed lines at $\pm x_s$. (b) Experimental phase space derived from the data shown in Fig. 6(b) (filled points) and phase space computed with the parameters $x_0=-0.15$ m, $\mu_s=0.32$, $\mu_k=0.25$, $\omega^2=24.5$ rad^2/s^2, and $\theta=1.44$ rad (dashed black line). Symmetrical centers are at $x_c=\pm 0.013$ m (continuous vertical lines), and the static region is delimited at $x_s\sim\pm 0.016$ m (dashed vertical lines). All six half oscillations are observed and good agreement is found between experimental and numerical data. [(c) and (d)] The ratio x_n/x_0 as a function of x_c/x_0 for $x_s/x_c=1$ (see Ref. 4) and $x_s/x_c=2$, respectively. The straight lines represent the final positions after an increasing integer number of half oscillations n. The slanted lines are shifted upward or downward because $x_s/x_c\neq 1$.

responding to the static region was measured, the linear damping of oscillations observed, and a detailed measurement of the final versus initial positions performed. The experimental results were discussed on the basis of the model according to which each half oscillation must have a center of symmetry. This model implies that two different centers of oscillations are obtained for upward and downward oscillations. The analysis led students to understand how static and kinetic friction forces act alternatively and how the cessation of the motion is due to the interplay of the two forces.

D. Using a numerical simulation

A numerical simulation based on the evaluation of the mass-spring system energy at each time step[4] can be useful to extend the experimental observations and to confirm the role of the static friction force in stopping the motion and the presence of two oscillation centers. If the students are directly involved in creating the simulation, they can explore the system using the point of view of energy as discussed in the Appendix. Students can also take advantage of the prewritten code to explore the simulated system and can quickly change the parameters to see the effect on the main physical quantities involved in the mass-spring system. The logical structure of the code is summarized in the Appendix.

IV. SUMMARY

We have proposed an approach for understanding the behavior of a harmonic oscillator in the presence of static and kinetic friction forces. The use of motion and force sensors makes the experimental analysis of a damped oscillator accessible to undergraduate and even to high school students. By using the experimental results as a starting point, the theoretical analysis can be discussed at a level of sophistication appropriate to the background of the students. For university students, it is advisable to combine experimental, analytical, and numerical approaches. In this way, we can explain a variety of observed phenomena. For example, the presence of two centers of oscillation can be explained as due to the periodic switch in the direction of the kinetic friction force after each half period, and the linear amplitude damping can be related to the magnitude of the kinetic friction force. A quantitative analysis of a plot of the final versus initial positions allows a direct estimate of the ratio of the friction coefficients of the block on the wooden plane.

ACKNOWLEDGMENT

The authors gratefully acknowledge the support of the Undergraduate Degrees in Science Project (Progetto Lauree Scientifiche) funded by the Italian Ministry of Education.

APPENDIX: PROGRAM

The code was written in FORTRAN and MATHEMATICA. The initial position x_0 and an initial zero velocity $v_0=0$ are chosen together with the parameters μ_s, μ_k, θ, and ω^2. The step size Δx is also chosen. The elastic spring force is compared to the static friction force to determine if mass oscillatory motion can begin. In the presence of motion, the subsequent position x_1 is related to the previous one by $x_1=x_0\pm\Delta x$, depending on the velocity direction. Then the velocity v_1 is evaluated by taking into account the work done by the kinetic friction force. If $v_1^2>0$, the updates of x and v are repeated until the velocity goes to zero, which is the first time the maximum amplitude is reached. This position becomes the new initial position. If, between the jth and the $(j+1)$th time steps, we find $v_{j+1}^2<0$, then the spatial resolution is increased until zero velocity is reached with the desired precision.

As a test of the program we compared our results with those obtained in Ref. 4. Figure 8(c) shows the ratio x_n/x_0 for different initial positions (in particular, $0\leq x_0/x_c\leq 20$) as a function of x_c/x_0 for $x_s/x_c=1$. Each straight line from right to left corresponds to a number of half oscillations increasing from 1 to 10. [For $0.3<x_c/x_0\leq 0.5$ shown in Fig. 8(c), one half oscillation was completed.] The first straight line (starting from the right) corresponds to one half oscillation, the second to two half oscillations, and so on; Fig. 8(d) shows the case $x_s/x_c=2$. Each straight line in Fig. 8(d) has the same slope as in Fig. 8(c), but is shifted upward or downward according to the number of half oscillations. This shift occurs due to the formation of a gap $2x_s-2x_c$, as shown in Fig. 2.

[1] U. Besson, L. Borghi, A. De Ambrosis, and P. Mascheretti, "How to teach friction: Experiments and models," Am. J. Phys. **75**, 1106–1113 (2007).
[2] H. Caldas and E. Saltiel, "Le frottement cinetique: Analyse des raisonnements des etudiants," Didaskalia **6**, 55–71 (1995).
[3] I. R. Lapidus, "Motion of a harmonic oscillator with variable sliding friction," Am. J. Phys. **52**, 1015–1016 (1984).
[4] I. R. Lapidus, "Motion of a harmonic oscillator with sliding friction," Am. J. Phys. **38**, 1360–1361 (1970).
[5] M. I. Molina, "Exponential versus linear amplitude decay in damped oscillators," Phys. Teach. **42**(8), 485–487 (2004).
[6] M. Kamela, "An oscillating system with sliding friction," Phys. Teach. **45**(2), 110–113 (2007).
[7] A. Marchewka, D. S. Abbott, and R. J. Beichner, "Oscillator damped by a constant-magnitude friction force," Am. J. Phys. **72**, 477–483 (2004).
[8] R. D. Peters and T. Pritchett, "The not-so-simple harmonic oscillator," Am. J. Phys. **65**, 1067–1073 (1997).
[9] C. Barratt and G. L. Strobel, "Sliding friction and the harmonic oscillator," Am. J. Phys. **49**, 500–501 (1981).
[10] PASCO Scientific, ⟨www.pasco.com⟩.

Information on a supplemental simulation for this article appears on the next page.

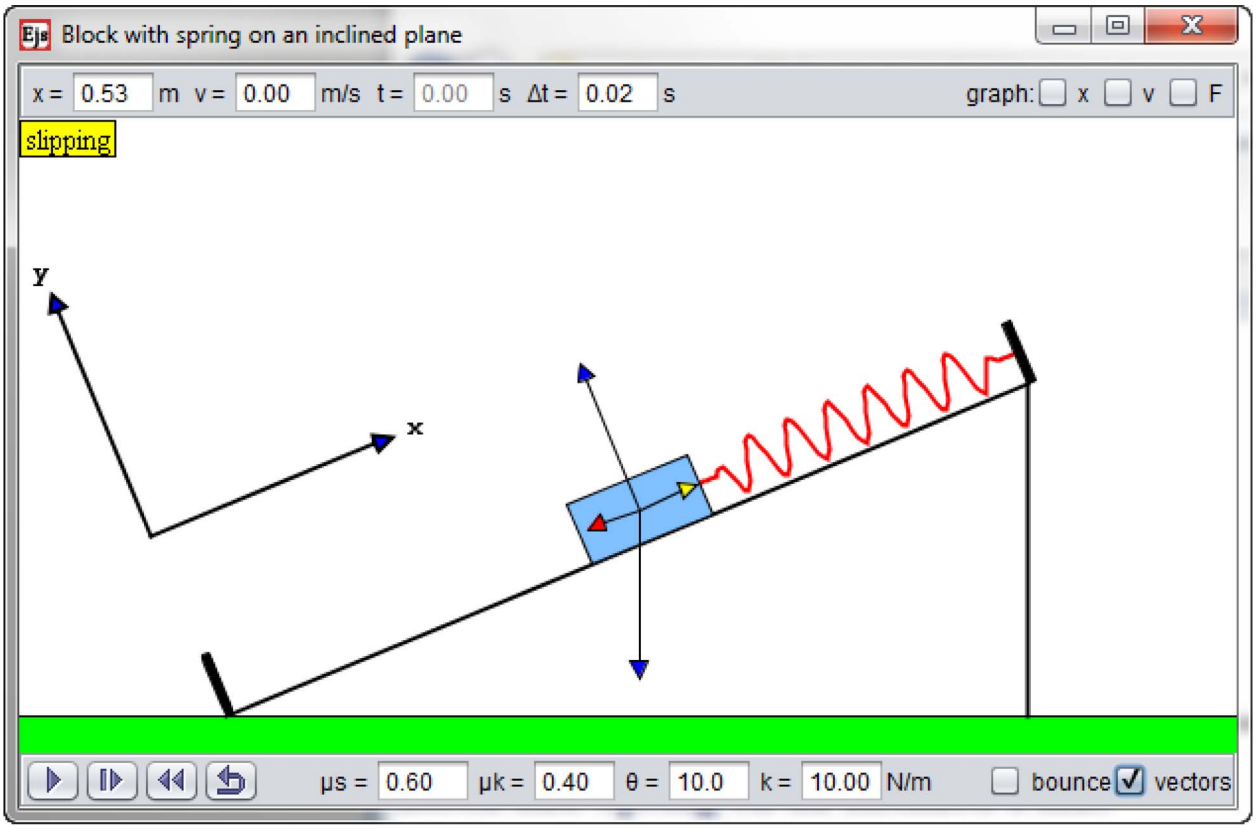

The Block and Spring on an Inclined Plane model in the OSP ComPADRE Collection shows the dynamics of a mass-spring system sliding on an inclined plane with static and kinetic friction. It is a supplemental simulation for the article by P. Onorato, D. Mascoli, and A. DeAmbrosis and has been approved by the authors and the AJP editor. The model displays the numerical solution to the equation of motion and shows how the forces change as the mass slides. Users can set the coefficients of friction and the spring constant. The model plots the position, velocity, and net force on the mass as a function of time as the system evolves and shows the asymmetry caused by the change in direction of the frictional force when sliding up and down the incline and the importance of friction in establishing equilibrium. The simulation can be found at http://www.compadre.org/OSP/items/detail.cfm?ID=10081.

Partial funding for the development of this model was obtained through NSF Grant No. DUE-0937731.

Wolfgang Christian